

**N 7 4 1 0 0 3 7**

**NASA TECHNICAL  
MEMORANDUM**

NASA TM X-71470

NASA TM X-71470

**CASE FILE  
COPY**

**NOISE TESTS OF A HIGH-ASPECT-RATIO SLOT NOZZLE  
WITH VARIOUS V-GUTTER TARGET THRUST REVERSERS**

by James R. Stone and Orlando A. Gutierrez  
Lewis Research Center  
Cleveland, Ohio 44135

TECHNICAL PAPER proposed for presentation at Eighty-sixth  
Meeting of the Acoustical Society of America  
Los Angeles, California, October 30-November 2, 1973

NOISE TESTS OF A HIGH-ASPECT-RATIO SLOT NOZZLE  
WITH VARIOUS V-GUTTER TARGET THRUST REVERSERS

by

James R. Stone and Orlando A. Gutierrez

Lewis Research Center  
National Aeronautics and Space Administration  
Cleveland, Ohio

ABSTRACT

The results of experiments on the noise generated by a 1.33- by 91.4 cm slot nozzle with various V-gutter reversers, and some thrust measurements are presented. The experiments were conducted with near-ambient temperature jets at nozzle pressure ratios of 1.25 to 3.0, yielding jet velocities of about 190 to 400 m/sec. At pressure ratios of 2 or less, the reversers, in addition to being noisier than the nozzle alone, also had a more uniform directional distribution and more high-frequency noise. At pressure ratios above 2, the nozzle alone generated enough shock noise that the levels were about the same as for the reversers. The maximum overall sound pressure level and the effective overall sound power level both varied with the sixth power of jet velocity over the range tested. The data were scaled up to a size suitable for reversing the wing-flap slot nozzle flow of a 45 400-kg augmentor-wing-type airplane on the ground, yielding perceived noise levels well above 95 PNdB on a 152-m sideline.

INTRODUCTION

Because short takeoff and landing (STOL) and reduced takeoff and landing (RTOL) aircraft are intended to operate from airports in heavily populated areas, they will be required to meet much stricter noise regulations than conventional aircraft. For this reason, the NASA Lewis Research Center has recently conducted several studies on the noise generated by STOL and RTOL propulsion system components including thrust reversers (refs. 1 to 3). One of the propulsive lift schemes being considered for such aircraft is the augmentor wing concept, in which the engine fan flow is ducted to the augmentor flaps, as illustrated in figure 1. A variation of this concept is also being considered for advanced supersonic transports. In order to reduce the ground roll of an augmentor-wing-type airplane, the wing-flap flow must be reversed, because its thrust is much greater than that of the core-engine exhaust jets. Both slot and multi-element nozzles are being considered for distributing the primary airflow along the augmentor flaps. Therefore, the noise generating characteristics of large-aspect-ratio thrust reversers for slot nozzles are required.

There have been numerous studies of the aerodynamic performance of small-size thrust reversers (e.g., ref. 4). However, studies of reverser noise

have been limited. (Refs. 1 and 2 deal with the core-jet target reversers, and ref. 3 presents noise data for a short (4.8 to 1) aspect ratio slot nozzle with a V-gutter reverser.) Scale up of the data of reference 3 to a 45 400-kg augmentor-wing-type STOL airplane indicated significant noise problems. Therefore, the present tests were conducted at larger scale and with higher, more realistic slot nozzle and reverser aspect ratio.

A V-gutter target-type reverser was chosen for this study, because such a configuration could be used with an augmentor-wing slot and flap system as shown in figure 1. The flap position at landing is shown in figure 1(a), and figure 1(b) shows how the two smaller flap sections could be moved to form a thrust reverser. The slot nozzle used was 91.4 cm long and 1.33 cm high, yielding an aspect ratio of 69. The isentropic nozzle jet velocity ranged nominally from 190 to 400 m/sec, corresponding to pressure ratios of 1.25 to 3.0. The effects of the following geometric variables were investigated: size of reverser, angle between reverser plates, spacing between nozzle and reverser, and offset of the reverser centerline from that of the nozzle. The effects of jet velocity and geometric variables on reverser noise are presented herein, with emphasis on the angle of maximum sideline noise. For one case, the data are scaled to a size suitable for reversing the wing flow of a 45 400-kg augmentor-wing-type airplane on the ground.

#### APPARATUS

The experimental data were obtained on two separate flow systems. The noise data were taken on an acoustic rig designed to minimize internal noise and instrumented to obtain detailed acoustic data. Another airflow rig was used to obtain exhaust-jet velocity surveys and data on flow coefficients and thrust-reversal efficiency. For the slot nozzle alone, the airflow rig was essentially as described in reference 5, but for the thrust reverser tests, the piping was extended far enough to let the existing velocity survey equipment be used in the reversed jets. Reverse thrust was measured by preloading the axial thrust load cell with 3.40 kN in weights hung from pulleys.

#### Acoustic Rig

The acoustic rig is shown in figure 2. Compressed air from a 1000-kN/m<sup>2</sup>-abs. source was supplied to the reverser at near ambient temperature ( $\sim 290$  to 300 K) by a 20-cm-diameter pipe. This pipe was equipped with a flow-measuring orifice, a remotely operated flow control valve, a noise muffler, and a straight run ending at the nozzle, which was 1.63 m above ground level. The reverser was attached to the nozzle by brackets.

The noise data were measured by eighteen condenser microphones with individual wind screens, located on two mutually perpendicular semicircles of 4.57-m radius centered on the middle of the nozzle exit plane. Nine of these microphones were spaced at 20° increments from  $\theta = 20^\circ$  to 180° from the pipe inlet centerline, at the same height above the smooth asphalt surface as the pipe centerline. These microphones are referred to as centerline-level. Eight microphones were mounted on an overhead boom, as shown in figure 2. The up-

stream axis of the pipe is at  $\theta = 0^\circ$ , and  $\theta = 180^\circ$  is the downstream extension of the pipe axis. Another microphone mounted on a stand at  $\theta = 180^\circ$  completed the  $20^\circ$ -to- $180^\circ$  vertical array. On the ground under this vertical microphone array was a 1-m-wide strip of 10-cm-thick acoustic foam to minimize reflections for the overhead array.

### Nozzles and Reversers

Slot nozzle. - The slot nozzle used in these studies is sketched in figure 3. The nozzle consists of a series of transition sections from the nominal 20-cm-diameter pipe to the 1.33-by 91.4-cm slot. The dimensions of the various transition sections are shown on the sketch. The rectangular cross-section portion of the nozzle is reinforced externally by steel angle. Internal support is provided by a 0.95-cm thick steel splitter plate with rounded leading edge and sharp trailing edge ending 6-cm upstream of the nozzle exit. A sheet metal fairing was added over the steel-angle supports back to the second support to provide a smooth surface for those cases where the reversed flow attached to the nozzle. This fairing can be seen in the photograph shown in figure 4(a). Some pertinent dimensions of the slot are

Slot height, $H_n$ , cm .....	1.33
Slot length, $W_n$ , cm .....	91.4
Slot area, $A_n$ , $m^2$ .....	0.0122
Aspect ratio, $W_n/H_n$ .....	68.7
Hydraulic diameter, $D_h$ , cm .....	2.63
Equivalent circular diameter, $D_e$ , cm .....	12.4

Reversers. - The reversers tested consisted of two flat, 0.64-cm thick steel plates, supported by steel angle, held in mounting racks, and clamped together. Figure 4(a) shows a photograph of a typical reverser configuration, showing its mounting rack and support structure. The reverser plates are 96.5-cm long, with widths  $L$  of either of 6.35 or 15.2 cm for the noise tests. The arrangement of the reverser with respect to the nozzle is sketched in cross-section in figure 4(b), and pertinent dimensions are defined. Plate angles,  $\alpha$ , were set at  $45^\circ$ ,  $52\frac{1}{2}^\circ$ , and  $60^\circ$ . Minimum spacings,  $Z_2$ , were varied from 0.95 to 6.35 cm and offset,  $Y$ , from 0 to 2.54 cm. One test was performed at  $\alpha = 90^\circ$ , which corresponded to a flat plate normal to the exhaust flow.

### PROCEDURE

The ranges of geometric variables for the acoustic tests were determined by prior tests on the airflow rig. Reverser positions were selected such that essentially full nozzle flow was obtained. Also before the slot nozzle and reverser acoustic tests were performed, a 10.2-cm diameter circular nozzle was tested on the acoustic rig. Tests were run with and without the foam ground mats to determine their effect on the sound measurements. The hori-

horizontal and vertical microphone arrays were then compared to obtain an estimate of the magnitude of ground reflections. The mats effectively eliminated the ground reflections at frequencies above 1000 Hz and reduced the ground reflections at lower frequencies.

#### Aerodynamic Tests

In order to assure that the noise tests were conducted at realistic reverser-to-nozzle spacings, the airflow rig was used to obtain data on flow and thrust-reversal efficiency. Typical effects of reverser-to-nozzle spacing on flow rate and reverse thrust for the larger-plate ( $L = 15.2$  cm) reverser at plate angle  $\alpha = 45^\circ$  are illustrated in figure 5. The ratio of flow rate to the flow rate for the nozzle alone at the same pressure ratio and temperature (reverse flow ratio) is plotted in figure 5(a) against the spacing between the nozzle outer lip and the reverser plates perpendicular to the plates ( $Z_1 = Z_2$ , fig. 4(b)). Similarly, the ratio of reverse thrust to forward thrust for the nozzle alone (thrust reversal efficiency) is plotted against the spacing in figure 5(b). In general for this case, as for the other spacings and plate angles, the flow rate increases fairly rapidly with spacing, approximately equaling the flow rate for the nozzle alone at a spacing  $Z_1 = Z_2 = 1.91$  cm. The thrust also increases with spacing at small spacing, but then decreases at large spacing, with a maximum also at about 1.91 cm. This is consistent with previous findings (ref. 4), in that for target reversers, the maximum thrust reversal efficiency occurs at the smallest spacing for which full nozzle flow is obtained.

#### Acoustic Tests

For each configuration, the nozzle inlet pressure was varied to give a series of nozzle pressure ratios, nominally 1.25, 1.40, 1.72, 2.00, 2.50, and 3.00. After flow conditions stabilized, flow parameters and atmospheric conditions were recorded and the noise data taken for each microphone. The noise data were analyzed directly by a 1/3-octave-band spectrum analyzer and recorded on magnetic tape for computer processing. The microphones were calibrated at the start and end of each running day with a standard piston calibrator. A variation up to  $\pm 0.5$  dB during the day was considered acceptable.

After the circular nozzle ground reflection tests were run, the slot nozzle was installed at an angle of  $45^\circ$  to the ground plane, and further ground-reflection data were obtained with and without the 1-m-wide foam ground mats. For the remainder of the tests, these ground mats were always used. The slot nozzle was then mounted in its normal horizontal position and baseline noise data obtained with and without the reverser mounting rack. Since no effects of the rack were observed, no further mention is made of this variable except to label such data on the figures. Next the 6.35-cm reverser plates were installed and  $\alpha$  and  $Z$  varied at  $Y = 0$ . Then the 15.2-cm reverser plates were installed and  $\alpha$ ,  $Z$ , and  $Y$  were all varied. (The ranges of variables is given in the Apparatus section.) In one case the plates were mounted at  $\alpha = 90^\circ$ , which represented the flat-plate, zero-reverse-thrust, limiting case.

## Acoustic Data Analysis

The 1/3-octave-band analyzer determined the sound pressure level SPL in each band from 50 to 20 000 Hz. These data were corrected for atmospheric absorption, and the overall sound pressure level OASPL was computed for each microphone. The effective spectral sound power level FWL and the effective overall (or total) sound power level OAPWL were obtained by integration. These power levels are termed "effective" since the noise measured may be a function of the azimuthal angle and the integration assumes symmetry about the jet axis.

### ground reflection

Detailed corrections are not made herein. The centerline-level microphones are corrected only for the high-frequency asymptotic reflection of 2.2 dB, and no correction is applied to the overhead microphones. Furthermore, no data falling within 5 dB of the upper limit of background noise at a given frequency are presented.

## RESULTS AND DISCUSSION

The noise data considered most significant in this investigation are presented herein in graphical form. For those requiring more detailed data, complete tables of 1/3-octave-band spectra are available, on request, from the authors.

### Slot Nozzle Noise

Noise data obtained with the slot nozzle alone are presented to provide a baseline for the reverser noise data, and also because the slot nozzle noise is of general interest itself. Data are presented for the nozzle in the normal position with the long axis parallel to the ground. The overall sound power levels were compared with the correlation of reference 6, which is based on conical and coaxial convergent-nozzle data from jet noise facilities thought to be reasonably free of extraneous noise sources. The present slot nozzle data, scaled in nozzle area and microphone geometry, are within the upper limit of the data used in developing the correlation of reference 6. This should verify that the facility is relatively free of extraneous noise sources especially for the reverser noise tests, where the noise levels, generally being higher, are further above any facility noise floor.

Effect of jet velocity on maximum sideline OASPL. - Figure 6 illustrates the dependence of the maximum sideline overall sound pressure level on the ground,  $OASPL_{max}$ , on the ideal isentropic jet velocity,  $U_j$ . The curve, to be used for comparisons, is simply faired through the experimental data. The subsonic, straight-line segment indicates an eighth-power dependence on velocity, i.e.,  $OASPL_{max}$  is proportional to  $10 \log U_j^8$ .

Spectra. - The sound pressure level spectra for the horizontal plane at the angle of maximum sideline OASPL (subsonic),  $\theta_{max} = 120^\circ$ , are shown in figure 7. For subsonic jet velocities, the data show no shift in peak-SPL frequency with changes in velocity. This is indicated by the fact that a single representative faired curve, shifted in level, but not in frequency,

can be selected for the various velocities. Similar results were also observed for all other angles tested. For the supersonic jet velocities tested, the sideline OASPL is slightly higher at  $\theta = 60^\circ$  due to dominant "screech" tones evident at that angle, but the broadband noise levels are highest at the subsonic  $\theta_{\max}$ .

The similarity of the spectra of figure 7 allows normalization of the subsonic data as shown in figure 8(a), where the normalized sound pressure level, SPL-OASPL, at the subsonic  $\theta_{\max}$  is plotted against the nondimensional frequency parameter,  $f_c D_h / c_a$ . The choice of hydraulic diameter,  $D_h$  as the significant dimension is based on comparisons of slot nozzle and circular nozzle data at  $\theta = 160^\circ$ , and should be considered arbitrary for the present case.

As with the SPL spectra, at subsonic jet velocities, the sound power level spectra for a given microphone geometry agree with the same faired curve, shifted in level, but not in frequency, for the various velocities. Similar results were shown for a circular nozzle in reference 7. The similarity of the PWL spectra allows normalization of the subsonic data as shown in figure 8(b), where the normalized effective sound power level, PWL-OAPWL, is plotted against the same nondimensional frequency parameter,  $f_c D_h / c_a$ , as was used for the SPL normalization.

#### Typical Effects of Thrust Reversal on Noise

Typical effects of thrust reversal on noise are presented in terms of the OASPL directivity and the SPL spectra at the angle of maximum sideline OASPL,  $\theta_{\max}$ , for the slot nozzle with and without reverser. The reverser consisted of the smaller plates ( $L = 6.35$  cm) at an angle  $\alpha = 45^\circ$ , spacing  $Z_1 = Z_2 = 1.91$  cm, and no offset. This configuration is the most similar to that of the smaller-scale, shorter-aspect-ratio reverser tests of reference 3. The data plotted are for a subsonic nozzle jet velocity  $U_j \approx 291$  m/sec, corresponding to a pressure ratio  $P_n/P_a \approx 1.72$ . The nozzle was mounted with its long dimension parallel to the ground.

OASPL directivity. - Figure 9 illustrates the typical effects of thrust reversal on the OASPL directivity. The most striking effect of thrust reversal is to increase the OASPL and make it more uniform in all directions. It is also quite important that the angle of maximum OASPL,  $\theta_{\max}$ , is shifted more toward the sideline with thrust reversal. These effects mentioned so far are consistent with the smaller-scale, shorter-aspect-ratio results of reference 3. Additional effects seen with the higher aspect ratio reverser are discussed, as follows. With and without the reverser, the noise levels are less in the plane of the nozzle long dimension (centerline-level) than in the overhead plane. These differences indicate a self-shielding effect due to the high aspect ratio. This self-shielding effect is greater with the reverser than with the slot nozzle alone. Also, both configurations show a greater variation of OASPL with  $\theta$  in the overhead plane than in the centerline-level plane.

Spectra. - The effect of thrust reversal on the SPL spectra at the angle of maximum sideline OASPL,  $\theta_{\max}$ , is shown in figure 10. The primary effect

of thrust reversal is to generate more high-frequency noise, thus shifting the peak-noise frequency to higher values. Again this is consistent with the shorter-aspect-ratio results (ref. 3). There is only a small effect of thrust reversal on the low-frequency SPL data.

#### Effect of Jet Velocity and Geometric Variables on Thrust Reverser Noise

Maximum sideline OASPL. - Figure 11 shows the dependence of the maximum sideline OASPL on jet velocity for the slot nozzle with V-gutter reversers at various spacings and plate angles. Data for the smaller-plate reverser ( $L = 6.35$  cm) configurations are shown in figure 11(a), with larger-plate ( $L = 15.2$  cm) data in figure 11(b). The reverser maximum OASPL is seen to increase with the sixth power of jet velocity, as first suggested by Curle (ref. 8) for the effect of solid boundaries on aerodynamic noise. Thus, at low jet velocities thrust reversal greatly increases the noise level, but at high jet velocities, where the nozzle alone exhibits considerable shock noise, the reverser can actually reduce the noise slightly. The effects of plate angle and spacing were insignificant over the range tested for the smaller-plate reversers (fig. 11(a)). The larger-plate data (fig. 11(b)) show the same trends as the smaller-plate data, although the effects of plate angle are greater. It is difficult to determine a consistent trend with plate height,  $L$ , at constant plate angle and spacing, but on the average the larger-plate reverser is a little louder.

The 6.35-cm spacing data (fig. 11(b)) are dominated by relatively low frequency tones. Since this large spacing also gives poor thrust performance, no further data at this spacing are presented. The  $\alpha = 90^\circ$  limiting case (fig. 11(b)), with zero reverse thrust, shows somewhat less noise than for smaller  $\alpha$ , where reverse thrust is obtained. Any further effects of plate angle are within the range of data scatter and are not considered significant. Some of the scatter for  $Z_1 = Z_2 = 1.91$  cm and  $\alpha = 52-1/2^\circ$ , may be partially due to a change in the reversed flow attachment from the nozzle fairing to the reverser plates, as indicated by exhaust jet surveys. For a plate angle  $\alpha = 52-1/2^\circ$ , offsetting the reverser apex from the nozzle exit center plane reduced the noise levels on the order of 3 or 4 dB at subsonic jet velocities, but the effect diminishes at supersonic jet velocities.

Spectra. - The sound pressure level spectra at the angle of maximum sideline OASPL for the smaller-plate reverser at plate angle  $\alpha = 52-1/2^\circ$  and spacings  $Z_1 = Z_2 = 1.91$  cm, which is taken to be a typical configuration, are shown in figure 12. The levels are above those of the nozzle alone (fig. 7) except at supersonic jet velocities, due to the fact that shock noise does not appear to effect the reverser spectra. Also, the peak-SPL frequencies are generally higher for the reverser. In contrast to the slot nozzle alone, the peak-SPL frequency increases slightly with increasing jet velocity. In order to normalize these spectra, the normalized sound pressure level, SPL-OASPL, is plotted against the nozzle Strouhal number based on equivalent diameter,  $f_c D_e / U_j$ , as shown in figure 13. Data for the two reverser configurations do not agree well for Strouhal number based on



$D_h$  (not shown), so the two sets of data are also compared based on  $D_e$ . The agreement based on  $D_e$  scaling is still not good, but is better than that based on  $D_h$  at low frequencies. Perhaps further analysis of the data will yield better scaling parameters. The other smaller-plate reverser configuration data agree quite well with the data of figure 13, and the larger-plate reverser data agree approximately with the smaller plate data.

The effective sound power levels normalize in a similar manner, as shown in figure 14 for the same configuration as in figures 12 and 13 as a typical example. The data for all the configurations tested agree fairly well with the faired curve. A faired curve for the V-gutter reverser of reference 3 is also shown, indicating only rough agreement with the present data.

#### Sideline Perceived Noise Levels at Aircraft Scale

An estimate of the sideline perceived noise levels for wing-slot flow reversal on a 45 400-kg augmentor-wing-type airplane was obtained from scaling of the experimental data for the quietest reverser configuration. The configuration chosen for scaling is the larger-plate reverser, with plate angle  $\alpha = 52\text{-}1/2^\circ$ , minimum spacing  $Z_2 = 0.95$  cm, and offset  $Y = 1.27$  cm. The data scaled are for a pressure ratio,  $P_h/P_a$ , of 2.50, or  $\sim 368$  m/sec jet velocity, which is in the range of interest for the augmentor-wing slot. The slot area was scaled up to give 84 kN ideal forward thrust which would correspond to one wing of the airplane. (It is assumed that the noise from only one of the wings would be heard.) Two different frequency-shift assumptions are applied: first, no shift is made in frequency, assuming that the slot height controls the frequency. This has the benefit of not requiring extrapolation to estimate the high-frequency data. Such an approach would be consistent with the observed trend for the slot nozzle data for frequencies to scale proportionally to  $1/D_h$ . Since the reverser noise frequencies scale better with  $1/D_e$ , this scaling assumption is also made. For the latter scaling assumption, it was necessary to extrapolate the experimental data to higher frequencies, for which a dropoff of 2 dB per 1/3-octave-band was assumed. No account was made for any reflection from the aircraft, but the ground reflections of the experimental data were included without correction. The data were corrected for atmospheric absorption according to reference 9; no correction was made for extra ground attenuation. The perceived noise level for each angle was then calculated according to reference 10.

The calculated noise levels are plotted in figure 15 against distance along the 152-m sideline on the ground. With either of the frequency scaling assumptions, the perceived noise levels are well above the 95-PNdB STOL design goal for a considerable distance along the sideline. As a point of reference, data scaled for the nozzle alone (no frequency shift) at the same 2.5 pressure ratio also indicate a maximum perceived noise level of  $\sim 107$  PNdB. Reducing the pressure ratio to 1.25 and increasing the nozzle area to obtain the same thrust as for the calculations of figure 15 would give a maximum perceived noise level of about 98 PNdB (again assuming no frequency shift in scaling). These results indicate that wing-slot thrust reversal with the type

of configurations tested would be a serious noise problem for STOL aircraft. Shielding was shown in reference 3 to have some potential for reducing the sideline noise for reversers of this type. Design modifications should also be investigated to determine whether or not the noise generated can be decreased.

#### SUMMARY OF RESULTS

The results of this experimental investigation of the noise generated by a 1.33- by 91.4 cm slot nozzle with and without various V-gutter target thrust reverser configurations may be summarized as follows:

1. The reversers generated more noise than the slot nozzle alone at subsonic jet velocities. At supersonic jet velocities, shock noise made the nozzle alone about as noisy as the reversers. In the plane of the nozzle long dimension, the noise directivity patterns for the reversers were more uniform than those of the slot nozzle alone.
2. In the plane of the nozzle long dimension, noise levels were lower than in the vertical plane perpendicular to it passing through the nozzle centerline, and were also lower than scaled-up data shorter-aspect-ratio reverser. These results indicate a self-shielding effect for high aspect ratio geometries in the plane of the nozzle long dimension. This effect is stronger with the reversers than for the slot nozzle alone.
3. For the reversers, the maximum OASPL and the effective sound power level both followed a sixth-power relation with isentropic jet velocity over the range tested (190 to 400 m/sec).
4. The sound pressure level spectra for the reversers were normalized as a function of nozzle Strouhal number based on equivalent circular diameter and isentropic jet velocity. The reverser geometry had no significant effect within the range of near-maximum reverse thrust. The sound pressure levels at each angle, as well as the effective sound power level, for each configuration, normalized in a similar manner.
5. For the slot nozzle alone, the sound pressure level spectra were normalized as a function of nozzle Strouhal number based on hydraulic diameter and ambient sonic velocity. The sound pressure levels at each angle, as well as the sound power level, normalized in a similar manner.
6. Test results, when scaled up to conditions suitable for reversing the wing thrust of a 45 400-kg augmentor-wing-type airplane, showed that noise levels could be significantly above the STOL design goal of 95 PNdB at the 152-m sideline.

#### SYMBOLS

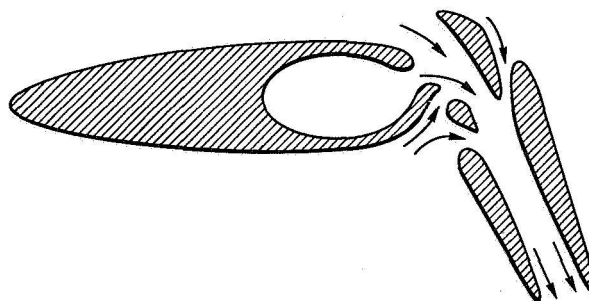
$A_n$	nozzle area, $m^2$
$c_a$	ambient speed of sound, m/sec

$D_e$	equivalent circular diameter, $\sqrt{4A_n/\pi}$ , m
$D_h$	hydraulic diameter, $4A_n/(\text{Nozzle perimeter})$ , m
$F_n$	nozzle forward thrust, N
$F_r$	reverse thrust, N
$f_c$	1/3-octave-band center frequency, Hz
$H_n$	nozzle slot height, m
$L$	height of reverser plate, m
$\dot{m}$	flow rate, kg/sec
$\dot{m}_n$	flow rate for nozzle alone, kg/sec
OAPWL	effective overall sound power level, dB re $10^{-13}$ W
OASPL	overall sound pressure level, dB re $20 \mu\text{N/m}^2$
$\text{OASPL}_{\text{max}}$	maximum sideline overall sound pressure level, dB re $20 \mu\text{N/m}^2$
$P_a$	ambient pressure, $\text{N/m}^2$ abs.
$P_n$	nozzle inlet total pressure, $\text{N/m}^2$ abs.
PNL	perceived noise level, PNdB
PWL	1/3-octave-band effective sound power level, dB re $10^{-13}$ W
SPL	1/3-octave-band sound pressure level, dB re $20 \mu\text{N/m}^2$
$U_j$	ideal isentropic, fully-expanded, jet velocity, m/sec
$W_n$	nozzle slot length, m
$Y$	offset of reverser apex from nozzle center plane, m
$Z_1$	spacing between nozzle outer lip and reverser, perpendicular to upper reverser plate, m
$Z_2$	spacing between nozzle outer lip and reverser, perpendicular to lower reverser plate, m
$\alpha$	angle between reverser plate and nozzle center plane, deg.

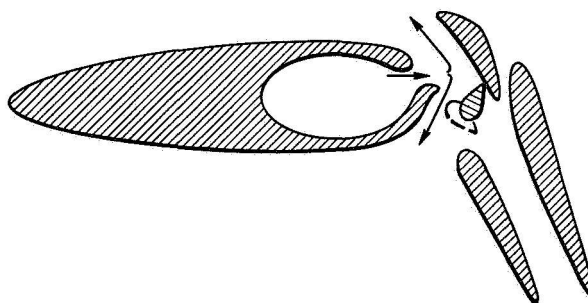
- $\theta$  angle of microphone to nozzle inlet axis, deg.
- $\theta_{\max}$  angle of maximum sideline OASPL, deg.

## REFERENCES

1. Gutierrez, Orlando A.; and Stone, James R.: Preliminary Experiments on the Noise Generated by Target-Type Thrust Reverser Models. NASA TM X-2553, 1972.
2. Stone, J. R.; and Gutierrez, O. A.: Target-Type Thrust Reverser Noise. J. Aircraft, Vol. 10, No. 5, May 1973, pp. 283-288.
3. Stone, J. R.; and Gutierrez, O. A.: Small-Scale Noise Tests of a Slot Nozzle with V-Gutter Target Thrust Reverser. NASA TM X-2758, 1973.
4. Povolny, John H.; Steffen, Fred W.; and McArdle, Jack G.: Summary of Scale-Model Thrust Reverser Investigation. NACA Rept. 1314, 1957.
5. Huff, Ronald G.; and Groesbeck, Donald E.: Splitting Supersonic Flow into Separate Jets by Overexpansion into a Multilobed Divergent Nozzle. NASA TN D-6667, 1972.
6. von Glahn, U. H.: Correlation of Total Sound Power and Peak Sideline OASPL from Jet Exhausts. Paper No. 72-643, AIAA, June 1972, (NASA TM X-68059).
7. Olsen, W. A.; Gutierrez, O. A.; and Dorsch, R. G.: The Effect of Nozzle Inlet Shape, Lip Thickness, and Exit Shape and Size on Subsonic Jet Noise. Paper No. 73-187, AIAA, Jan. 1973.
8. Curle, N.: The Influence of Solid Boundaries Upon Aerodynamic Sound. Proc. Royal Soc. (London) A231, 1955, pp. 505-514.
9. Anon: Noise Standards: Aircraft Type Certification. Federal Aviation Regulations, Vol. III, Part 36, 1969.
10. Anon: Definitions and Procedures for Computing the Perceived Noise Level of Aircraft Noise. Aerospace Recommended Practice 865A, SAE, Aug. 15, 1969.



(A) TYPICAL LANDING CONFIGURATION.



(B) POSSIBLE SLOT REVERSER CONFIGURATION, V-GUTTER TYPE.

Figure 1. - Augmentor wing slot-flow reversal scheme.

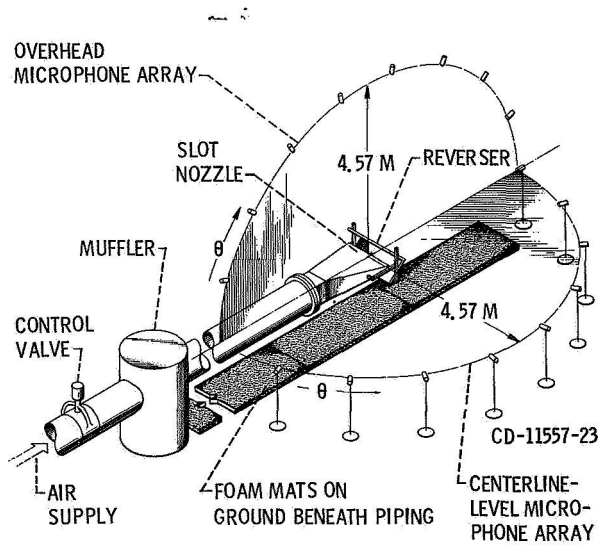


Figure 2. - Acoustic rig schematic diagram.

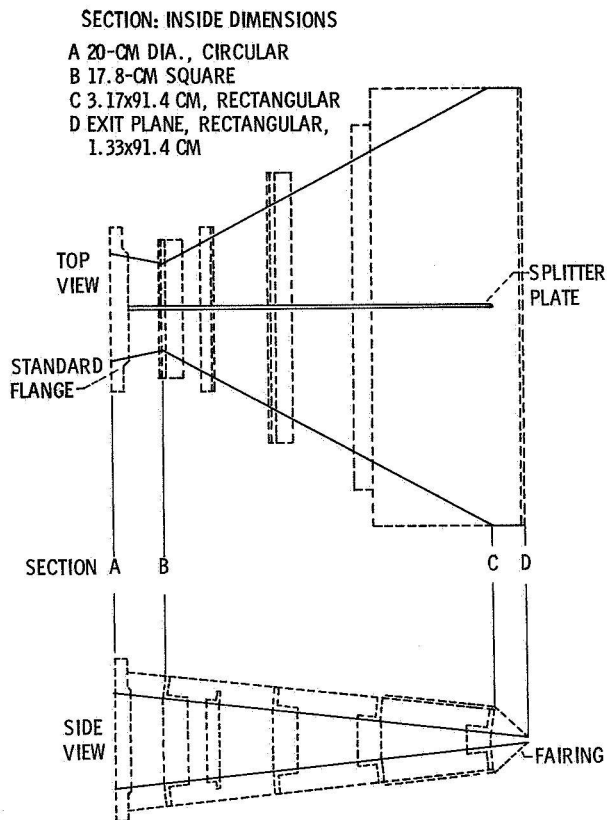
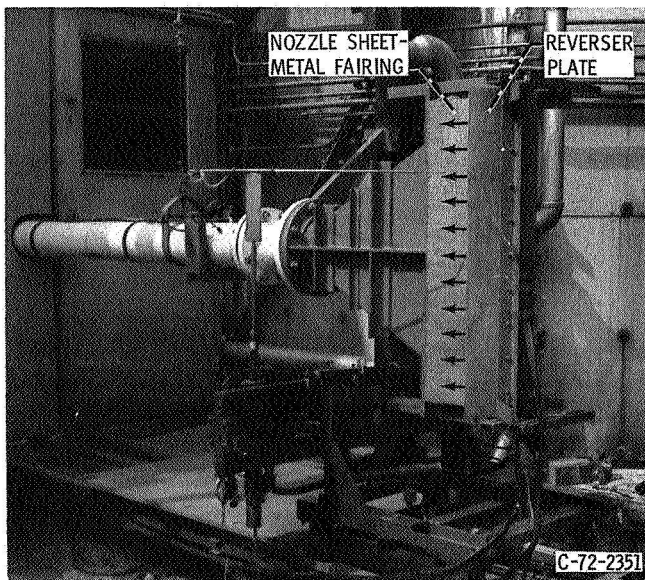
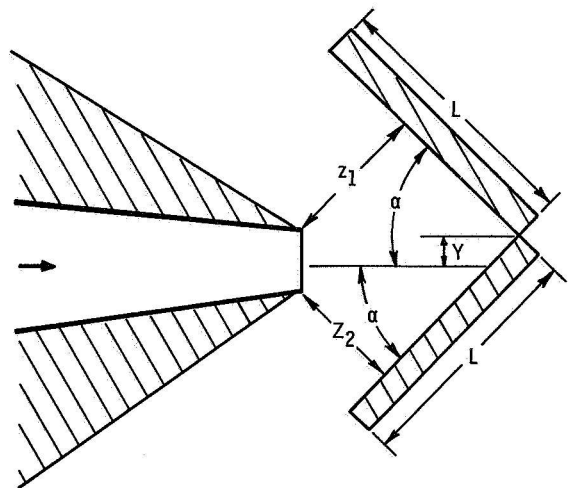


Figure 3. - Slot nozzle sketch (flow passage, solid lines; support structure, dashed lines).



(a) PHOTOGRAPH OF INSTALLATION IN AIRFLOW RIG.



(b) SKETCH SHOWING GEOMETRIC VARIABLES.

Figure 4. - Arrangement of nozzle and reverser.

NOZZLE PRESSURE RATIO,

$P_n/P_a$   
 1.40  
 1.73  
 2.00  
 2.50  
 3.00

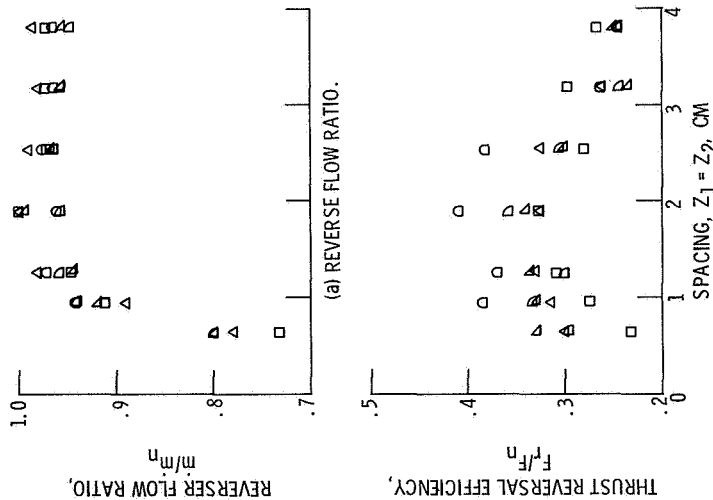


Figure 5. - Effect of spacing on flow rate and reversing thrust for 1.33-by-91.4-cm slot nozzle with larger-plate V-gutter reverser (L = 15.2 cm), at plate angle  $\alpha = 45^\circ$ .

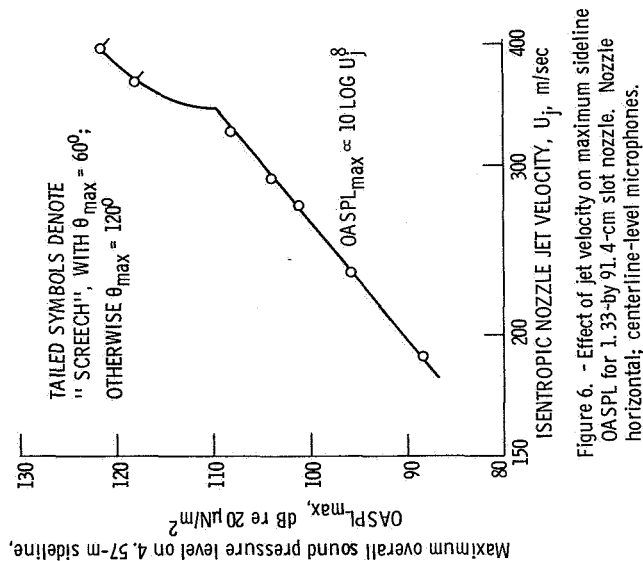


Figure 6. - Effect of jet velocity on maximum sideline OASPL for 1.33-by-91.4-cm slot nozzle. Nozzle horizontal; centerline-level microphones.

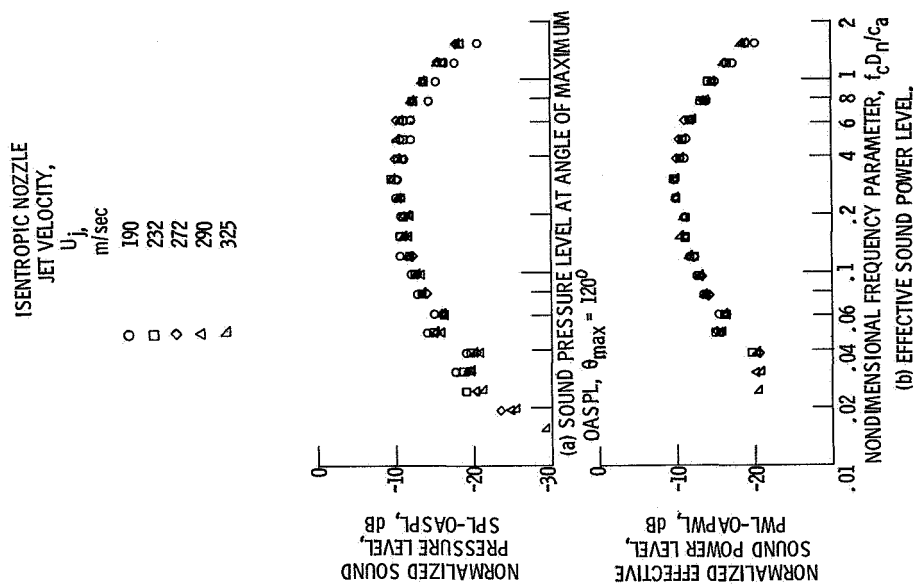


Figure 8. - Normalized subsonic spectra for slot nozzle alone. Nozzle horizontal; centerline-level microphones.

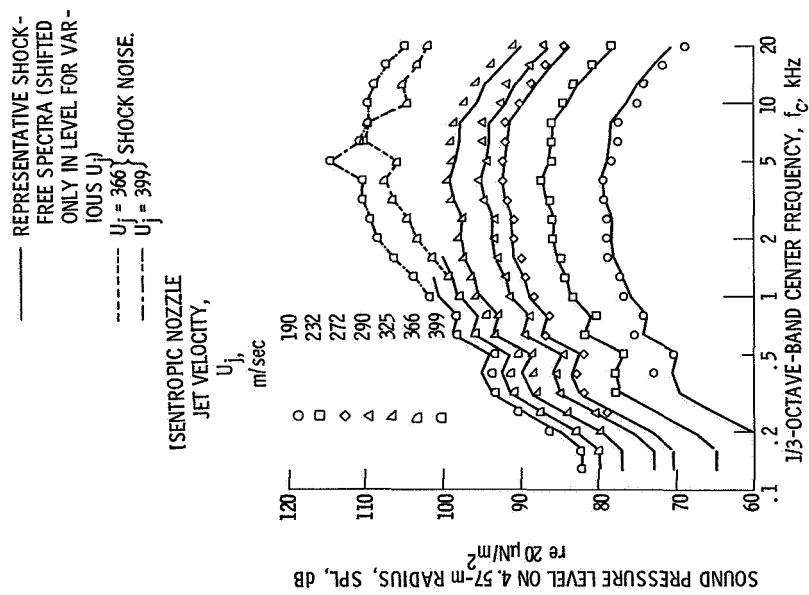
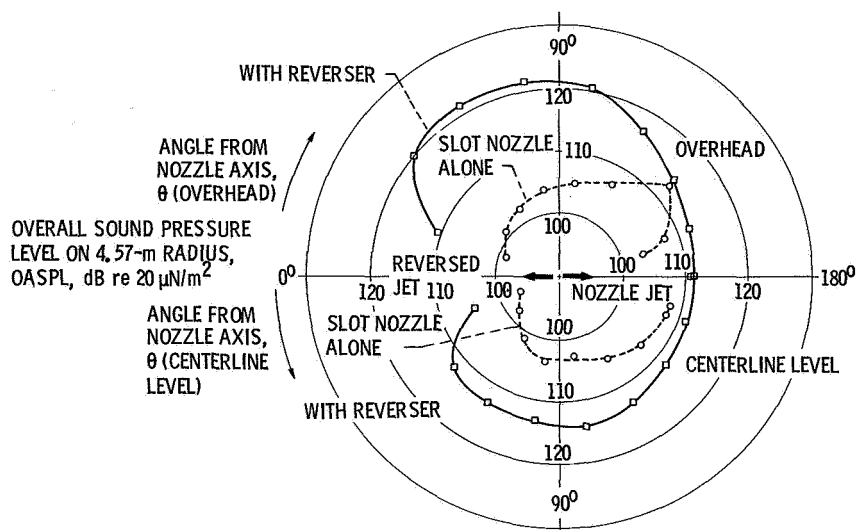


Figure 7. - Sound pressure level spectra for 1.33-by-91.4-cm slot nozzle at angle of maximum subsonic OASPL,  $\theta_{\max} = 120^\circ$ . Nozzle horizontal; centerline-level microphones.





(a) DIRECTIVITY OF OVERALL SOUND PRESSURE LEVEL.

Figure 9. - Effect of thrust reversal on directivity of overall sound pressure level for 1.33-by 91.4 cm slot nozzle and typical V-gutter reverser ( $L = 6.35$  cm,  $\alpha = 45^\circ$ ,  $Z_1 = Z_2 = 1.91$  cm,  $Y = 0$ ). Nozzle jet velocity,  $U_j \sim 291$  m/sec. Long dimension parallel to ground.

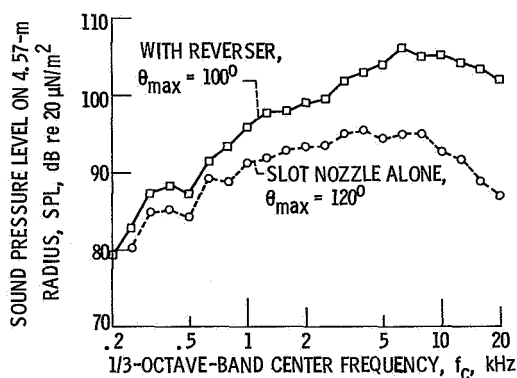


Figure 10. - Effect of thrust reversal on SPL spectra at angle of maximum sideline OASPL for slot nozzle and typical reverser;  $L = 6.35$  cm;  $Z_1 = Z_2 = 1.91$  cm,  $Y = 0$ ,  $\alpha = 45^\circ$ , Nozzle jet velocity,  $U_j \sim 291$  m/sec; nozzle and reverser horizontal; centerline-level microphones.

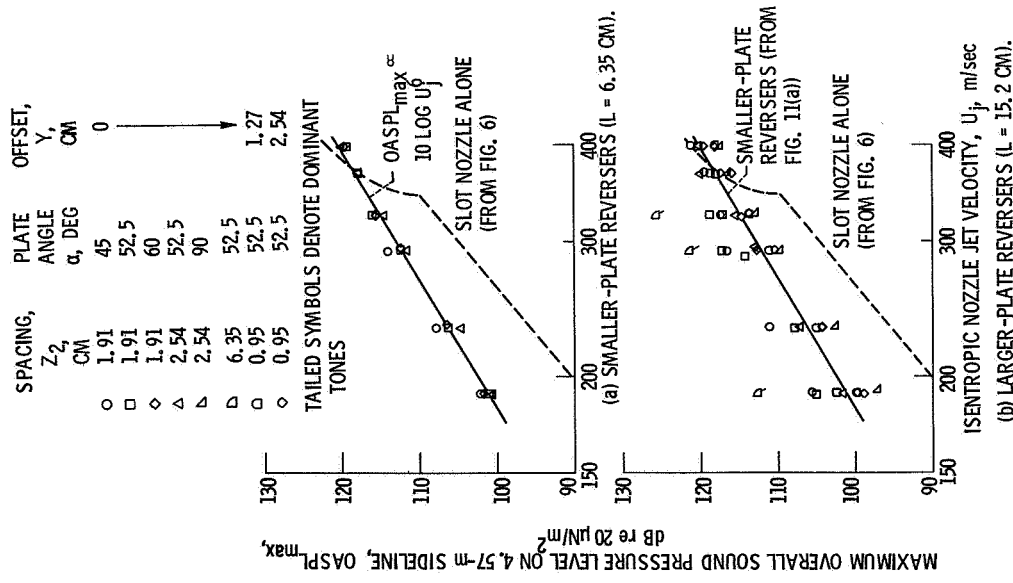


Figure 11. - Effect of jet velocity on maximum sideline OASPL for various V-gutter reversers. Nozzle and reverser horizontal; centerline-level microphones.

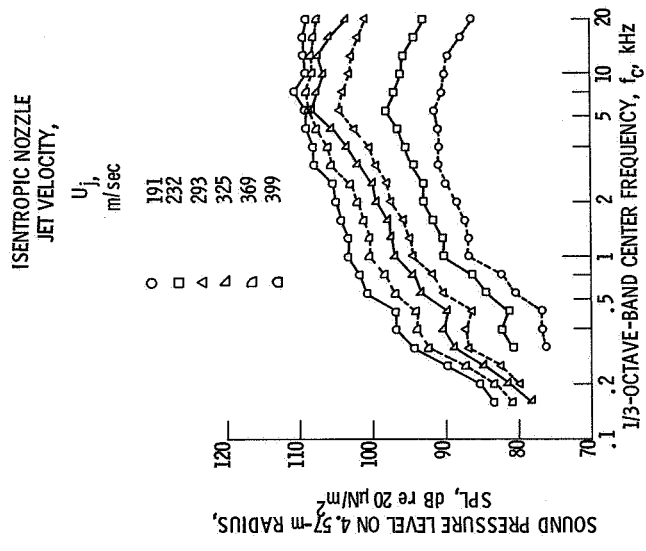


Figure 12. - Sound pressure level spectra at angle of maximum sideline OASPL,  $\theta_{max} = 100^\circ$ , for slot nozzle with smaller-plate V-gutter reverser ( $L = 6.35$  cm) with spacing  $Z_1 = Z_2 = 1.91$  cm and plate angle  $\alpha = 52-1/2^\circ$ . Nozzle and reverser horizontal; centerline-level microphones.

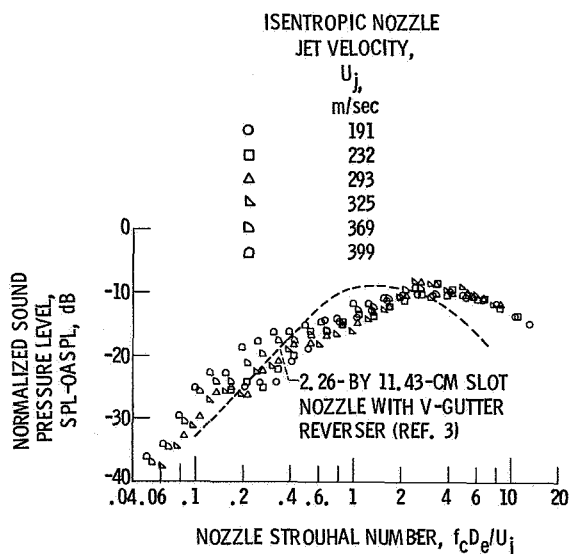


Figure 13. - Normalized sound pressure level spectra at angle of maximum sideline OASPL,  $\theta_{\max} = 100^\circ$ , for slot nozzle with smaller-plate V-gutter reverser ( $L = 6.35$ -cm) with spacing  $Z_1 = Z_2 = 1.91$  cm and plate angle  $\alpha = 52\text{-}1/2^\circ$ . Nozzle and reverser horizontal; centerline-level microphones.

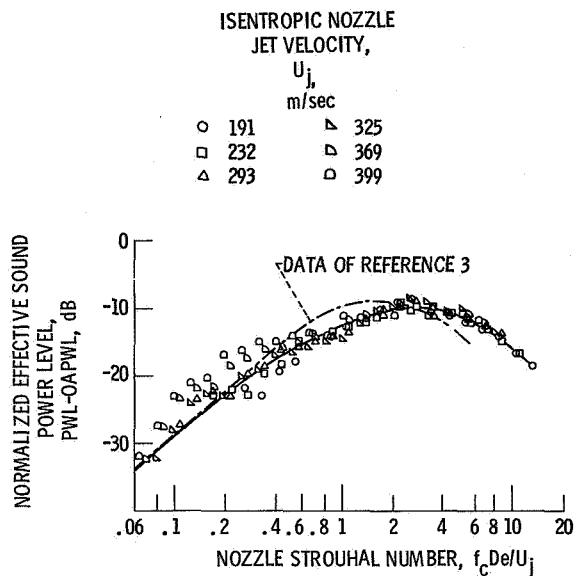


Figure 14. - Normalized effective sound power level spectra for slot nozzle with smaller-plate V-gutter reverser ( $L = 6.35$  cm) with spacing  $Z_1 = Z_2 = 1.91$  cm and plate angle  $\alpha = 52\text{-}1/2^\circ$ . Nozzle and reverser horizontal; centerline level microphones.

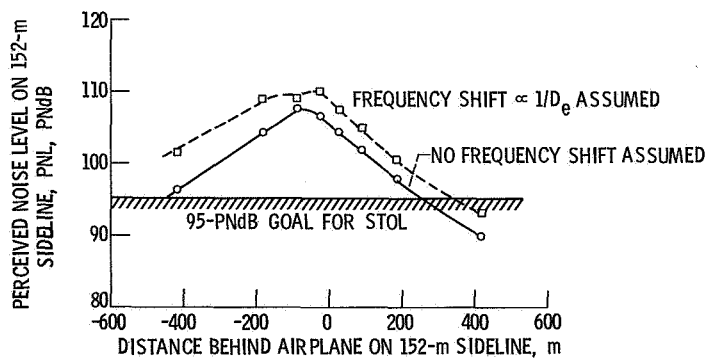


Figure 15. - Sideline noise for wing-slot thrust reversal on 45 400-kg augmotor-wing-type airplane. Slot nozzle pressure ratio, 2.5; jet velocity,  $U_j$ , 362 m/sec. Noise from one wing.